Meas. Sci. Technol. 10 (1999) 1127–1134. Printed in the UK PII: S0957-0233(99)03885-0

Quantifying seabed properties in shelf waters using a parametric sonar

Paul C Hines

Defence Research Establishment Atlantic, PO Box 1012, Dartmouth, Nova Scotia, Canada B2Y 3Z7

E-mail: hines@drea.dnd.ca

Received 30 April 1999, in final form and accepted for publication 20 July 1999

Abstract. Defence Research Establishment Atlantic is developing a bottom-tethered, wide-band sonar for collecting acoustic data in the open ocean. The transmitter, a parametric array, offers three advantages: a wide bandwidth (1–10 kHz), a narrow beamwidth (≈3°) and virtually no sidelobes. These features allow direct measurement of seabed parameters in shallow water. Direct in this context means the absence of complications resulting from unwanted interactions of the acoustic pulse with ocean boundaries. This makes the parametric sonar an ideal tool with which to interrogate the seabed in shelf waters and quantify several geo-acoustic properties. To complement the narrow-beam active sonar, a six-channel superdirective/intensity array has been developed for the receiver. The superdirective receiver obtains a significantly narrower beam for a given array aperture than that obtained using a conventional acoustic receiver. A 900 MHz rf command link is used to steer the array to any combination of azimuth and tilt angle. Together with control over azimuth and tilt angle, the sonar frame is instrumented to monitor depth, roll and vertical acceleration to ensure quality control of the data. Data transmission back to the ship is accomplished via a 2.3 GHz rf data link capable of a data-transfer rate of up to 8 Mbits s^{-1}. This paper describes the system's technical functionality, its acoustic principles of operation and its measurement application.

Keywords: acoustic intensity, acoustic pressure, parametric array, superdirective array, intensity array, acoustic scattering, bottom loss

1. Introduction

Quantifying the effect that the seabed has on an acoustic wave is crucial if one is to assess the performance of current sonar systems. Furthermore, advances in sonar technology require a clear understanding of how sound interacts with the seabed. This includes reflection and scattering from, as well as penetration into, the seabed. We require direct measurements of these parameters that are unhindered by vertically directed sidelobes which generate unwelcome fathometer returns. In deep water this is accomplished by locating the sonar sufficiently near the seabed to temporally separate signals of interest from the fathometer returns; however, in shallow coastal water at low kilohertz frequencies this isn't possible. This is because the size of a conventional sonar is roughly proportional to its acoustic wavelength and, in order to project a sufficiently narrow acoustic beam, the sonar must be many wavelengths long. In this circumstance, one can't place the sonar near enough to the seabed.

To address this deficiency the Defence Research Establishment Atlantic (DREA) is developing a bottom-tethered, wide-band active sonar (WBS) with which to interrogate the seabed and quantify its geo-acoustic properties. The sonar's direction is remotely controlled from a research ship via a rf radio link. This minimizes the risk of acoustic interference from the ship and prevents ship motion from compromising array stability. Figure 1 is a schematic diagram of the configuration.

A parametric array was chosen for the acoustic source. The parametric array—the principles of which will be outlined later in the paper—offers three advantages. First and foremost, due to the nature of signal generation in the parametric array, no sidelobes are formed. This feature avoids the added complexities of boundary interactions when making measurements in shallow water. This allows one to measure, for example, the reflection and scattering characteristics of the seabed in the absence of interference from sonar sidelobes. Second, one can obtain a wider bandwidth than that obtained using a conventional source. In the present case a bandwidth of 1–10 kHz is realized from a single transducer. The wide bandwidth means that a single transducer can be used in place of a suite of transducers, each of which may require separate power and tuning circuitry. The wide bandwidth also allows a great deal of flexibility in the types of pulses available. Third, the beamwidth of the parametric array is extremely narrow relative to the transmitter aperture. In the present case a square transducer measuring 41 cm on a side yielded horizontal and vertical beam widths of approximately 3°. The price paid for these advantages is poor acoustic efficiency—approximately 0.1–1.0% across the difference-frequency band.

© 1999 Canadian Government

101-02323/

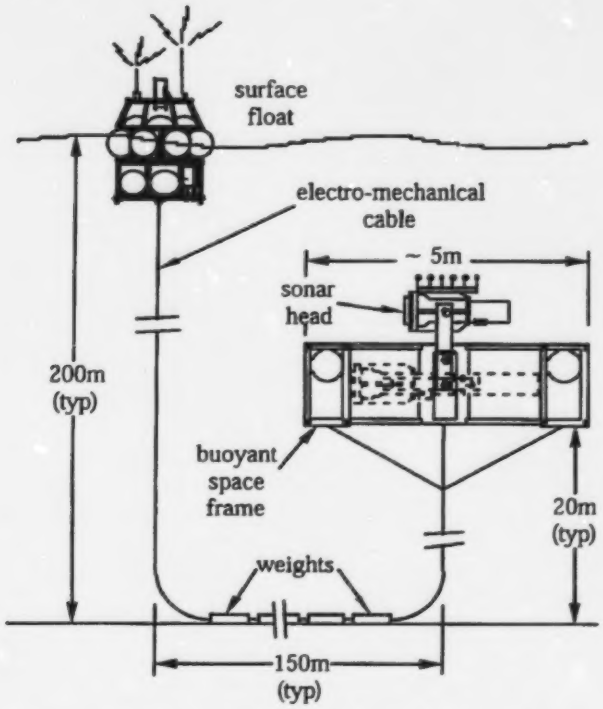

Figure 1. A schematic diagram of the Wide Band Sonar (WBS) showing the surface float, electromechanical cable, space frame and sonar head.

To complement the compactness of the parametric transmitter, a six-channel superdirective/intensity line array of hydrophones was developed for the receiver. This type of array relies on computing pressure gradients and as such requires inter-element spacings that are a small fraction of an acoustic wavelength. Thus, by its very nature, a superdirective/intensity array is much more compact than a conventional array. The principal disadvantage with a 'difference array' is its susceptibility to incoherent noise such as sensor self-noise and inter-channel phase errors. That is to say, the very process of taking the difference between the acoustic signals at two sensors means that the signal-to-noise ratio (SNR) must be degraded.

In conjunction with the acoustic sensors, the array is instrumented with a range of non-acoustic sensors to evaluate the quality of the data. The non-acoustic sensors include depth, tilt, roll and heading sensors to monitor the array position and direction, as well as accelerometers to monitor platform vibration. Platform stability is maintained through a bottom-mounted de-coupling configuration which prevents surface wave motion from degrading the sonar's performance. The system is bottom-tethered rather than free-drifting so as to maintain control over the experimental geometry.

Following the introduction, an overview of the WBS system and its technical functionality is given. Then its acoustic principles of operation are presented in detail. Finally, the main applications of the WBS to seabed measurements are highlighted.

2. An overview of the system

As shown in figure 1, the WBS consists of a surface buoy, a weighted electro-mechanical cable and a positively buoyant sub-sea space frame. The space frame holds the transmitter and receiver and acts as the support structure for electronic cans and battery packs. An electronic compass, two inclinometers and four accelerometers are mounted on the space frame to monitor the platform orientation and vibration, respectively. The system is designed to ensure platform stability, a key factor in the performance of the sonar.

Since the sonar is designed to project a narrow acoustic beam, the positioning system must permit it to accurately acquire an acoustic target and the platform must provide sufficient directional stability to hold that target until an echo is received. A series of hydraulic actuators driven by an electro-hydraulic servo system achieves the former requirement; a bottom-tethered platform, streamed into the prevailing shear current, satisfies the latter.

The sub-surface space frame consists of tubular aluminium pipe. Sub-surface floats are positioned to make the space frame positively buoyant with its top surface horizontal. The sonar head is mounted on an arm that nests the sonar inside the space frame to protect it from damage during deployment and recovery. Once it has been deployed, the arm projects the head below or above the space frame as desired. The head can then be steered to any combination of azimuth and elevation to permit coverage of a complete hemisphere.

The space frame is connected to a surface float via an armoured electro-mechanical cable, with ancillary weights over part of its length. The weighted portion, which lies along the bottom, serves two purposes; it sets the height to which the buoyant platform will rise and it isolates the platform from motions of the surface float.

The surface float supports the upper end of the electro-mechanical cable and houses battery packs and electronics that allow rf communication between the research vessel and the sonar. There are two rf links. The first is a one-way UHF data link operating at 2.3 GHz which is used to transmit the acoustic and non-acoustic data back to the ship. The second is a two-way UHF command link operating at approximately 900 MHz which is used to maintain system control. A more detailed discussion of the mechanical and electrical specifications of the WBS is contained in [1]. The system has undergone an open-ocean engineering trial as well as acoustic calibration trials in an indoor tank [2] and on DREA's acoustic calibration barge in Halifax harbour [3].

3. Acoustic principles of operation

3.1. The parametric array transmitter system

Guigné International Limited (GIL) of St John's, Newfoundland was commissioned by DREA to design and construct a high-power, low-frequency parametric array. The parametric array, referred to as Parametric Array Transmit System (PATS), serves as the transmitting head in the WBS.

The fundamental principles of the parametric array were first presented in a paper by Westervelt [4], in which he described the nonlinear interaction of sound in water and

the subsequent generation of sound at frequencies other than those transmitted. Briefly, if two intense sound beams are coaxially transmitted into water, the nonlinearity of the water medium generates secondary frequencies which are the sum and difference of the primary propagation frequencies. In practical applications, absorption attenuates the sum frequency at small distances from the transmitter and it is the difference frequency which is of principal interest. The sound-pressure level and the beam pattern at the difference frequency are complicated functions of the transducer aperture and source level, the choice of primary and difference frequencies and the properties of the medium. The literature contains a plethora of useful references on the theory of operation of parametric arrays as well as their application to the study of acoustic penetration into the seabed. See for example, Muir *et al* [5], Williams *et al* [6], Maguer *et al* [7], Moffett and Mellen [8] and the references therein. Moffett and Mellen state that the operating regime of a parametric array can approach one of four limits. These limits depend on whether the array length is terminated by small-signal absorption or nonlinear absorption and whether array termination occurs in the near-field or the far-field of the primary beam. For the present case, the array is near-field limited and approaches the limit of nonlinear absorption.

There are several unique properties of the parametric array that make it attractive for the present system. First and foremost, the difference-frequency wave has no sidelobes. This feature is particularly useful for shallow-water measurements since it prevents interference from unwanted boundary interactions. For example, this allows backscattering measurements at shallow grazing angles without interference from sidelobe fathometer returns. Secondly, the difference frequency has a much narrower beamwidth than could be obtained by generating the same signal with a conventional transducer. This allows one to construct a narrow-beam source operable in shallow water whose vertical dimension is much less than the water-column depth. Figure 2 shows a cross-section of the beam pattern as a function of the angle, ψ_d, measured at a difference frequency of 4 kHz. There is no evidence of sidelobes out to ±45° and the two-sided half-power beamwidth is less than 2°. The third advantage in using a parametric array is that a low Q is achieved at the difference frequency. In essence, the bandwidth at the primary frequency is translated down to the difference-frequency band. In the case of PATS, this offers a usable bandwidth of greater than 10 kHz at the difference frequency. Wide-band sources of this type are ideal for interrogating the fine structure within the seabed [9].

The parametric transmitter consists of nine square piston transducers made of PZT-4 ceramics arranged in a 3-by-3 grid. The active area is approximately 0.11 m^2 for the nine-transducer array. At full power, the primary source level is 242 dB re 1 μPa at 1 m range, at 100 kHz. The pulse duration can range from 50 μs to 250 ms. The minimum pulse duration is limited by the receiver bandwidth and the maximum is limited by the heat dissipation of the PZT-4 ceramic. The main disadvantage in employing a parametric array is that the conversion of energy from the primary frequencies to the difference frequency is a second-order process and therefore inefficient. Table 1 lists the sound-pressure level (SPL_d) measured at 16 m and the inferred source level (SL_d) referred to 1 m range for a selection of difference frequencies. Also shown in table 1 are the beamwidths measured at several difference frequencies.

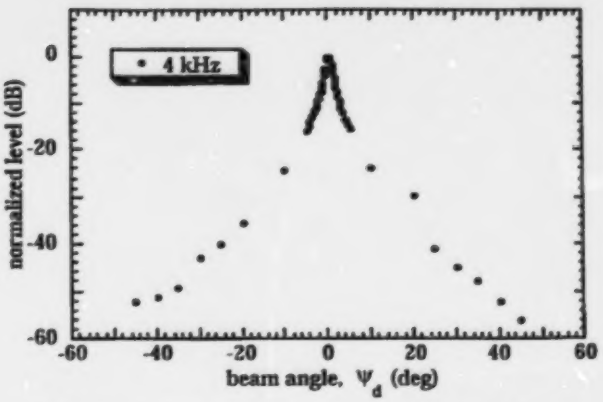

Figure 2. The difference-frequency beam pattern measured at 4 kHz. Note that there is no evidence of sidelobes out to at least ±45° and the two-sided half-power beamwidth is less than 3°.

Table 1. Difference-frequency source levels and sound-pressure levels (SL_d and SPL_d, respectively) and difference-frequency beamwidths. The sound-pressure levels were measured at 16 m range and the beamwidths were measured at 10 m range. The SL_d, referred to 1 m range, were computed from the measured SPL_d by assuming spherical spreading. (The measured source levels are approximately 3 dB below the maximum achievable due to limitations of the peak voltage on the transmit amplifiers. Minor alterations to the circuitry will correct this. The examples shown in section 4.1 assume source levels 3 dB greater than those shown in this table.)

f_d (kHz)	SL_d (dB re 1 μPa @ 1 m)	SPL_d (dB re 1 μPa)	−3 dB beam (degrees)
1.0	166	142	n/a
2.0	173	149	1.7
4.0	180	156	1.8
8.0	188	164	2.2
10.0	191	167	n/a

3.2. The superdirective/intensity receiver evaluation module (SIREM)

Given the acoustical inefficiency of parametric arrays, a high-gain, yet compact receiver is needed for the WBS. Conventional line arrays form acoustic beams using the principle of time delay and summation [10] to align the signal received at each sensor. This causes the (coherent) signal to reinforce and the (incoherent) ambient noise to average out. This design benefits from large inter-element spacings since the signal tends to have a greater coherency length than does the noise. In contrast, superdirective and intensity hydrophone arrays estimate pressure gradients of various orders by taking the difference between signals received at pairs of sensors and normalizing by the sensor spacing. Since this technique approximates the gradient, the inter-element spacing must be much less than a wavelength. Thus, by its very nature, the superdirective/intensity array is much more

compact than the conventional array. Superdirective and intensity arrays based on pressure sensors require essentially the same hardware specifications; the difference between them lies in how one processes the signals received [11]. In the first case one obtains the intensity by *multiplying* pressure and pressure-gradient signals; the superdirective solution is obtained by *summing* the pressure and the pressure gradient. The measurement environment dictates which solution is better for a given experiment. It is interesting to note that, in a conventional array, gain occurs against ambient noise if the noise is *incoherent* since it will then average out; however, in a difference array, gain occurs only against *coherent* noise. One achieves gain against ambient noise with the difference array because the ambient noise is coherent at small inter-element spacings.

The principal disadvantage of these 'difference arrays' is that theoretical gains are difficult to achieve due to their susceptibility to uncorrelated noise. This can include pre-amplifier voltage noise, inter-channel imbalance in gain and/or phase, sensor-spacing errors, acoustic scattering and hydrophone self-noise due to hydrodynamic flow past the sensors. Voltage noise and inter-channel imbalance can be minimized through careful design of pre-amplifiers and modern digitization techniques. Sensor-position errors are reduced by compliantly mounting the hydrophones onto stiff mounting rods. Flow noise can be reduced by enclosing the hydrophones in an acoustically transparent shroud such as open-cell foam. Finally, noise resulting from scattering can be minimized by ensuring that hardware in the vicinity of the hydrophones is of sufficiently low-profile design. The last constraint is perhaps the most difficult to quantify and it is often the quality of the data which determines whether the design requirement has been met. Modelling [12] indicates that, in the absence of sensor noise, a six-hydrophone array with an aperture of 0.8 m will provide approximately 15 dB gain against three-dimensionally isotropic ambient noise.

The SIREM is a six-channel difference-array receiver used in the WBS system. The hydrophones have a nominal acoustic sensitivity of -200 dB re 1 V μPa^{-1}. The pre-amplifiers were custom-built by GIL. The GIL pre-amplifiers have a 12 dB fixed gain at the input stage with 60 dB additional gain selectable in 12 dB increments. The dynamic range of the pre-amplifier varies from a high of 150 dB at the 12 dB gain setting to a low of 100 dB at the 72 dB gain setting. At 1 kHz, the inter-channel phase matching of the hydrophone/pre-amplifier is better than $\pm 0.25°$ and the pre-amplifier noise (referred back to the input) is less than -165 dB V Hz$^{-1/2}$ at all gain settings. The hydrophones are positioned on one spine of the PATS head so as to sit proud of the transducer by 20 cm. Inter-channel spacing can be varied from 6 to 16 cm with positional accuracy better than 1 mm. Although SIREM has been designed to quantify the processing gains of the two 'difference-array' methods, results reported in this paper will be limited to receiver gains using superdirective processing.

The directivity of an nth-order superdirective line array is given by [12]

$$D_g(\varphi) = \left(\frac{\sum_{n=0}^{M} w_n G(n) / \left[2j \sin\left(\frac{kd}{2}\right) \right]^n}{\sum_{n=0}^{M} w_n} \right)^2 \qquad (1)$$

where k is the acoustic wavenumber, d is the inter-element spacing, $j = \sqrt{-1}$ and φ is the spherical–polar angle depicted in figure 3. The term $G(n)$ is an approximation to the nth-order pressure gradient for a unity-gain signal and is given by

$$G(n) = j^n 2^n \sin^n \left(\frac{kd \cos\varphi}{2} \right) \qquad (2)$$

and w_n is a weighting factor applied to the nth-order gradient. The weights are chosen to optimize the gain against the specific noise field of interest. One begins by expressing the noise gain NG as

$$NG = \frac{\int_0^{2\pi} d\theta \int_0^{\pi} d\varphi \sin\varphi D_g(\varphi) N_a(\theta, \varphi)}{\int_0^{2\pi} d\theta \int_0^{\pi} d\varphi \sin\varphi N_a(\theta, \varphi)} \qquad (3)$$

where $N_a(\theta, \varphi)$ is the ambient-noise directionality function and φ and θ are angles in the spherical–polar coordinate system shown in figure 3. To minimize NG one differentiates equation (3) with respect to each of the unknown weights and sets the result to zero. This yields M simultaneous equations in M unknowns which are solved for the weights. The array gain AG is given by

$$AG = SG/NG \qquad (4)$$

where the signal gain $SG = 1$, as noted above. For the case of a six-element array in three-dimensionally isotropic noise we have $M = 5$, $N_a(\theta, \varphi) = 1$ and $w_{n3D} = \{1, 7, -14, -42, 21, \frac{231}{5}\}$. With this weighting scheme one obtains $AG = 36$ (15.6 dB) in the limit of $d \to 0$. Franklin points out that, in actual fact, one is usually better off choosing a weighting scheme optimized for two-dimensionally (i.e. horizontally) isotropic noise due to its robustness in the presence of self-noise and channel imbalance. Furthermore, optimizing the weights for a two-dimensionally isotropic noise field and employing them in a three-dimensionally isotropic noise field results in less than a 0.5 dB reduction in array gain. Noting this, calculations in this paper will be based on measurements made in a three-dimensionally isotropic noise field with weights optimized for two-dimensionally isotropic noise. The two-dimensional weights for a six-element array are given by

$$w_{n2D} = \{1, 6, -12, -32, 16, 32\}. \qquad (5)$$

Figure 4 shows the idealized superdirective array gain in dB (AG_{dB}) plotted as a function of kd, for $M = 5$, $N_a(\theta, \varphi) = 1$ and w_{n2D} given by equation (5). The array gain decreases with increasing kd because the approximation to the gradient degrades. This defines the high-frequency operating limit of the superdirective array. The low-frequency limit of the superdirective array arises when one includes the effects of uncorrelated noise. This is addressed next.

3.3. The effect of system noise on a superdirective array

As noted earlier, the principal disadvantage of difference arrays is that theoretical gains are difficult to achieve at low frequency due to their susceptibility to uncorrelated system noise. In SIREM, voltage noise limits the array's performance. To quantify its effect we note from Franklin

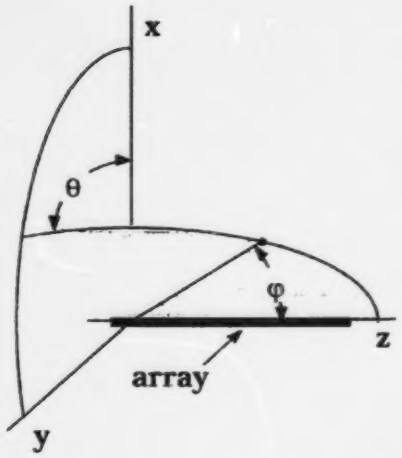

Figure 3. The spherical–polar coordinate system oriented such that the array is aligned with the z axis. Although it is somewhat unconventional, this orientation simplifies the integration in equation (3).

[12] that the degradation in array gain AD due to uncorrelated noise can be written as

$$AD = 1 + \frac{N_{sn}}{N_0 NG} \qquad (6)$$

where N_0 is the ambient noise power and N_{sn} is the system noise. The system noise at the output of a superdirective line array, N_{sn}, is given by [12]

$$N_{sn} = N_s\left[\left(\sum_{i=1}^{M/2} \frac{w_{2i}(-1)^i {}_{2i}C_i}{W(-p^2)^i}\right)^2 + 2\left(\sum_{i=1}^{M/2} \frac{w_{2i}(-1)^{i+1} {}_{2i}C_{i+1}}{W(-p^2)^i}\right)^2 + 2\left(\sum_{i=2}^{M/2} \frac{w_{2i}(-1)^{i+2} {}_{2i}C_{i+2}}{W(-p^2)^i}\right)^2\right] + \cdots$$
$$\cdots N_s 2\left[\left(\sum_{i=1}^{\overline{M/2}} \frac{w_{2i}(-1)^i {}_{2i}C_i}{W(-1)^{i-1}p^{2i-1}}\right)^2 + 2\left(\sum_{i=1}^{\overline{M/2}} \frac{w_{2i-1}(-1)^{i+1} {}_{2i-1}C_{i+1}}{W(-1)^{i-1}p^{2i-1}}\right)^2\right] + \cdots \qquad (7)$$

where N_s is the system noise power of an individual pre-amplifier, ${}_aC_b$ is the binomial coefficient for the $(b+1)$st term, $W = \sum_{n=0}^{M} w_n$, $p = 2\sin(kd/2)$ and $\underline{M/2}$ and $\overline{M/2}$ represent the summations taken to the floor and ceiling of the fraction, respectively.

In order to quantify the effect of voltage noise on array performance, one must first compute the voltage response of the hydrophone/pre-amplifier for a specific ambient-noise data set. This is compared with the voltage noise of the pre-amplifier. By way of example figure 5 shows ambient noise collected on Western Bank off the coast of Nova Scotia (full line) [13]. The data were collected in water 60 m deep during winds of 20 knots. The measured data are limited to below 2 kHz; the data have been extrapolated to 10 kHz by assuming a roll-off of 6 dB per octave. The left-hand vertical axis shows the data in units of dB re 1 μPa Hz$^{-1/2}$, whereas the right-hand vertical axis provides the conversion to dB V Hz$^{-1/2}$. Also plotted in figure 5 (as a broken line) is the voltage-noise background of an individual pre-amplifier (N_s). Using figure 5 and equations (6) and (7) one can estimate the array degradation as a function of frequency and, from that, adjust the theoretical array gain shown in figure 4 to obtain the corrected receiver-array gain. To convert the data of figure 5 into wavenumber space one must of course specify the inter-element spacing d.

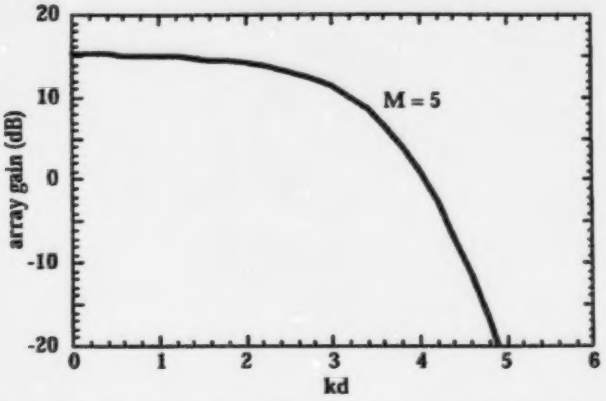

Figure 4. The idealized superdirective-array gain in dB (AG_{dB}) plotted as a function of kd, for a fifth-order superdirective array in a three-dimensionally isotropic ambient noise field.

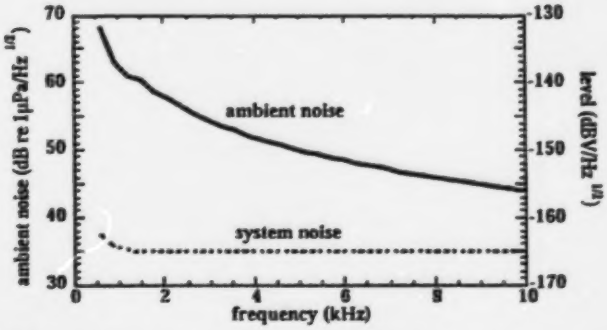

Figure 5. The ambient noise collected in 60 m water off the coast of Nova Scotia (full line). The measured data are limited to below 2 kHz; the data have been extrapolated to 10 kHz by assuming a roll-off of 6 dB per octave. The left-hand vertical axis shows the data in units of dB re 1 μPa Hz$^{-1/2}$, whereas the right-hand vertical axis provides the conversion to dB V Hz$^{-1/2}$. Also plotted (as a broken line) is the voltage-noise background of an individual pre-amplifier, N_s.

Figure 6 shows the corrected array gain in decibels, AG_{cdB}, for a six-hydrophone array with an inter-element spacing of 16 cm. A pair of curves is used because, for any Mth-order array, system noise results in negative array gain outside some frequency pass band. This pass band is a function of the array order and inter-element spacing. Employing array orders of $M = 5$ and $M = 2$ provides adequate gain up to 5 kHz, above which the transmitted source level is sufficient to provide ample SNR using a single hydrophone. Since increasing the hydrophone spacing

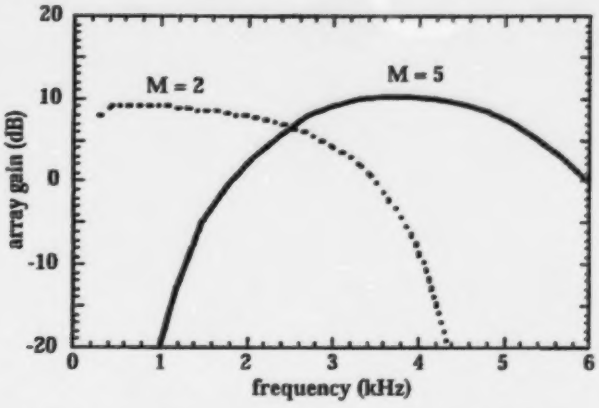

Figure 6. A pair of curves for the array gain corrected for noise (AG_{cdB}) for a six-hydrophone array with an inter-element spacing of 16 cm. Employing array orders of $M = 5$ and $M = 2$ provides adequate gain up to 5 kHz, above which the transmitted source level is sufficient to provide ample SNR using a single hydrophone.

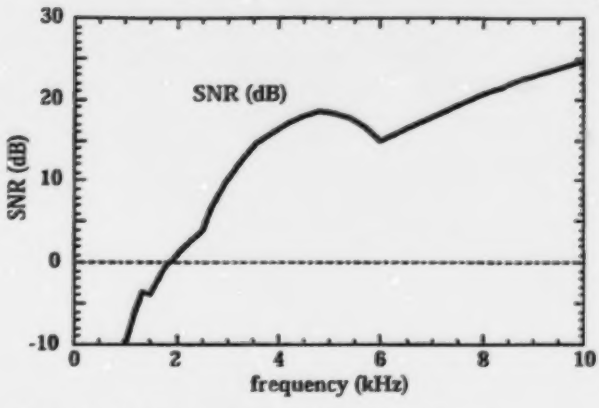

Figure 7. The signal-to-noise ratio (SNR) for a sample experimental scenario in which one wants to measure the backscattering strength of the seabed at a shallow (10°) grazing angle.

improves the array performance at low frequency, the spacing is doubled to $d = 32$ cm (by using every second hydrophone) for the $M = 2$ case.

4. Application to seabed measurements

4.1. Measuring the backscattering strength of the seabed

One of the primary applications of the WBS is to measure the backscattering strength (BSS) of the seabed at shallow (i.e. sub-critical) grazing angles. Therefore, it is reasonable at this point to estimate the system's SNR for a typical experimental scenario. We assume that the WBS lies at a height h, 20 m above a seabed in an isovelocity ($c = 1500$ m s^{-1}) water column. Furthermore, we assume a pulse length of $\tau = 20$ ms, directed at a grazing angle of $\phi_g = 10°$. Under these conditions one obtains for the insonified area, A, a value of

$$A = \Delta y \Delta z \approx R\psi_r[c\tau/(2\cos\phi_g)] \tag{8}$$

where ψ_r is the difference-frequency beamwidth measured in radians ($\psi_r \approx 0.05$ rad) and $R = h/\sin(\phi_g)$ is the slant range from the source to the scattering patch. Finally we shall assume a backscattering strength of $BSS = -45$ dB. To estimate the SNR we re-cast the sonar equation in terms of the SNR by writing

$$\text{SNR} \equiv \text{RL}_d - N_0 + 10\log_{10}(1/\tau) = \text{SL}_d - 40\log_{10}(R) + BSS + 10\log_{10}(A) + AG_{cdB} - N_0 + 10\log_{10}(1/\tau) \tag{9}$$

where the received level RL_d, the ambient noise N_0, the source level SL_d, the backscattering strength BSS and the array gain of the receiver AG_{cdB} are defined on a decibel scale and the term $10\log_{10}(1/\tau)$ is a bandwidth correction to convert the ambient-noise contribution from a per-hertz band (shown in figure 5) to the bandwidth of a pulse of duration τ. Equation (9) ignores the effect of absorption which is minimal at these frequencies and ranges.

Figure 7 shows the SNR calculated using equation (9) and plotted as a function of frequency. The frequency-dependent source level is approximated by interpolating the values in table 1, AG_{cdB} is obtained from figure 6 and N_0 is obtained from figure 5. For frequencies greater than approximately 2500 Hz the SNR exceeds 5 dB.

4.2. Bottom-classification techniques

The parametric array's ability to produce short pulses—and therefore wide-bandwidth coherent signals—makes it an excellent tool for investigating the fine structure of the seabed. In this section a qualitative example is presented to provide some insight on this application. First, we note that the primary pressure field $p_p(t)$ can be described as an amplitude-modulated carrier. In this example we employ a normalized pulse of the form

$$p_p(t) = 0.5[1 + \cos(2\pi f_m t)][\cos(2\pi f_p t)] \quad \text{for } -T/2 < t < T/2 \tag{10}$$

where f_m and f_p are the modulation and primary frequencies, respectively, and the difference frequency $f_d = 2f_m$. Berktay [14] shows that the far-field difference-frequency pressure field $p_d(t)$ is given by

$$p_d(t) = \kappa \frac{\partial^2}{\partial t^2} E^2(t) \tag{11}$$

where $E(t) = 0.5[1 + \cos(2\pi f_m t)]$ is the envelope of the primary pressure wave and κ is a constant related to the nonlinearity of the medium. Figure 8 shows a plot of $E(t)$ and $p_d(t)$ for $f_m = 4$ kHz, $f_p = 100$ kHz and a pulse duration of $\tau = 250$ μs. Figure 9 shows the power spectrum of $p_d(t)$ which has a bandwidth of approximately 5 kHz. (Note that replacing the envelope given in equation (10) by a square envelope would increase the difference-frequency bandwidth at the expense of some loss in efficiency [15]).

Once again we assume that the WBS lies at a height h, 20 m above the seabed in an isovelocity water column, with a sound speed of $c = 1500$ m s^{-1}. Positioning the sonar at normal incidence will result in an insonified area

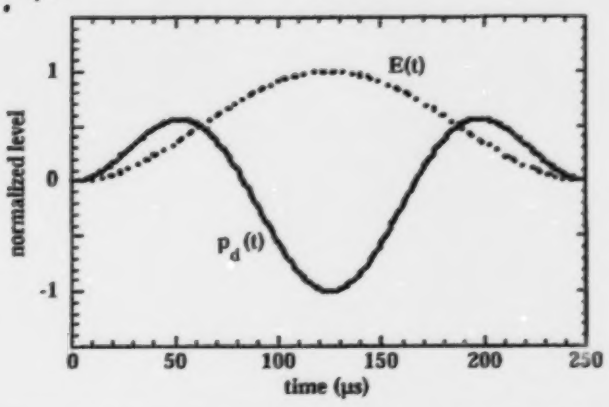

Figure 8. A plot of the envelope function $E(t)$ (broken line) and the difference-frequency waveform $p_d(t)$ (full line) for a transmitted pulse given by equation (10) with $f_m = 4$ kHz, $f_p = 100$ kHz and $\tau = 250$ μs.

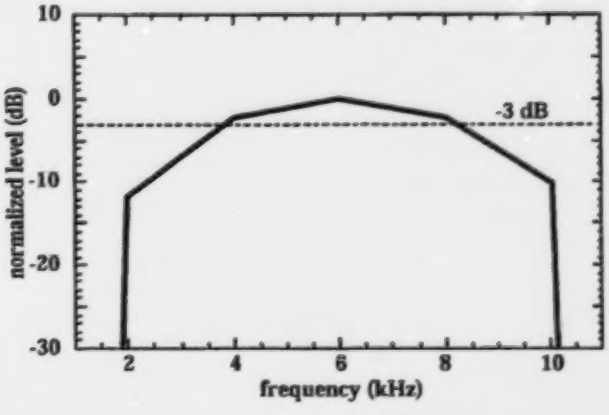

Figure 9. A plot of the power spectrum of $p_d(t)$ from figure 8.

$A \approx 1$ m^2, with a vertical resolution of $c\tau/2 \approx 0.20$ m. If one employs the match-filter processing technique of Guigné *et al*, the frequency content of the returns can be used to distinguish among different types of bottom. At this difference frequency, absorption in sediments is typically of the order of 1 dB m^{-1} [16]. Therefore, the source levels from table 1 will provide adequate SNR on scattered/reflected returns from the sub-bottom down to tens of metres depth. Finally, one could double the modulation frequency and halve the pulse length, thereby doubling the bandwidth and the depth resolution, at the expense of a decrease in penetration depth.

5. Conclusions

The WBS has been designed to provide a versatile platform from which to conduct environmental acoustic measurements of ambient noise and backscattering from the ocean surface and the seabed, as well as to interrogate the fine structure within the seabed using wide-bandwidth coherent impulses. Using a parametric transmitter prevents sidelobes from contaminating measurements via unwanted boundary interactions and keeps the dimensions of the acoustic system small. Employing a superdirective/intensity array for the receiver constrains its physical dimensions as well since, by its very nature, this type of array is much more compact than a conventional array. These features make the system ideal for making measurements in littoral waters.

The parametric array provides a difference frequency source level ranging from 166 to 191 dB re 1 μPa at 1 m range across the 1–10 kHz band. The superdirective/intensity receiver provides array gains of 10–15 dB. Together these systems provide sufficient SNR to allow backscattering measurements down to at least 10° grazing angles over most seabeds.

The parametric array's wide bandwidth and low frequency are ideally suited to interrogating the fine structure of the seabed. Its wide bandwidth provides high spatial resolution whereas its relatively low difference frequency permits penetration deep into the bottom.

Another key feature of the system is that the sonar's direction is remotely controlled from a research ship via a rf radio link. This permits a wide range of experimental geometries, minimizes the risk of acoustic interference from the ship and prevents ship motion from compromising array stability.

Acknowledgments

The author wishes to acknowledge invaluable technical input by Mr W Cary Risley, Mr Martin P O'Connor, Mr Donald Mosher, Mr Paul Shouldice, Mr Bryce Davis, Mr Robert Cushing and Mr Roger Arsenault.

References

[1] Hines P C, Cary Risley W and O'Connor M P 1998 A wide-band sonar for underwater acoustics measurements in shallow water *Proc. Oceans '98, Nice, September 29–November 1*

[2] Hamm C A and Hines P C 1998 Measurements and modelling on a high-power, low frequency parametric array *Proc. Institute of Acoustics Symp. on Underwater Acoustic Calibration and Measurements, National Physical Laboratory, Teddington, July 20–21*

[3] Hines P C and Hamm C A 1999 Calibration of a high-power, low-frequency, parametric array designed for ocean environments *Proc. 15th Int. Symp. on Nonlinear Acoustics, Gottingen, September 1–4*

[4] Westervelt P J 1963 Parametric acoustic array *J. Acoust. Soc. Am.* **35** 535–7

[5] Muir T G, Thompson L A, Cox L R and Frey H G 1980 A low-frequency parametric research tool for ocean acoustics *Bottom-Interacting Ocean Acoustics* ed W A Kuperman and F B Jensen (New York: Plenum) pp 467–83

[6] Williams K L, Satkowiak L J and Bugler D R 1989 Linear and parametric array transmission across a water-sediment interface—theory, experiment, and observation of beam displacement *J. Acoust. Soc. Am.* **86** 311–25

[7] Maguer A, Bovio E, Fox W L J, Pouliquen E and Schmidt H 1998 Mechanisms for subcritical penetration into a sandy bottom: experimental and modelling results SACLANTCEN, Italy, SACLANT Undersea Research Centre Report SR-287 (April 1998)

[8] Moffett M B and Mellen R H 1977 Model for parametric acoustic sources *J. Acoust. Soc. Am.* **61** 325–37

[9] Guigné J Y, Schwinghamer P and Liu Q 1993 High resolution and broadband processing of acoustic images of the marine benthos *Conf. Proc. Acoustic Classification and Mapping of the Seabed* vol 15 part 2
[10] Urick R J 1975 *Principles of Underwater Sound* 2nd edn (New York: McGraw-Hill) p 51
[11] Franklin J B 1997 Intensity measurements and optimum beamforming using a crossed dipoles array *DREA* CR/97/443
[12] Franklin J B 1997 Superdirective receiving arrays for underwater acoustic application *DREA* CR/97/444
[13] Hazen M and Desharnais F 1997 The eastern Canadian shallow water ambient noise experiment *Conf. Proc., Oceans '97* vol 1, pp 471–6
[14] Berktay H O 1965 Possible exploitation of nonlinear acoustics in underwater transmitting applications *J. Sound Vibration* **2** 439–61
[15] Merklinger H M 1975 Improved efficiency in the parametric transmitting array *J. Acoust. Soc. Am.* **58** 784–7
[16] Clay C S and Medwin H 1977 *Acoustical Oceanography: Principles and Applications* (New York: Wiley-Interscience) p 259

#513110